Brain Research 1694 (2018) 38–45

Contents lists available at ScienceDirect

Brain Research

journal homepage: www.elsevier.com/locate/bres

Research report

Bilateral thalamocortical abnormalities in focal cortical dysplasia

Arthur Rezayev [a,b], Henry A. Feldman [c], Jacob Levman [b,d,e], Emi Takahashi [b,e,*]

[a] Department of Biology, Boston University, 5 Cummington Mall, Boston, MA 02215, USA
[b] Division of Newborn Medicine, Department of Medicine, Boston Children's Hospital, Harvard Medical School, 300 Longwood Avenue, Boston, MA 02115, USA
[c] Clinical Research Center, Boston Children's Hospital, Harvard Medical School, 300 Longwood Ave, Boston, MA 02115, USA
[d] Department of Mathematics, Statistics and Computer Science, St. Francis Xavier University, Antigonish, NS B2G 2W5, Canada
[e] Athinoula A. Martinos Center for Biomedical Imaging, Massachusetts General Hospital, Harvard Medical School, Charelestown, MA 02219, USA

ARTICLE INFO

Article history:
Received 4 December 2017
Received in revised form 3 May 2018
Accepted 4 May 2018
Available online 5 May 2018

Keywords:
Focal cortical dysplasia
Diffusion tensor imaging
White matter
Epilepsy
Pediatric

ABSTRACT

Background and purpose: Focal cortical dysplasia (FCD), a congenital malformation of the neocortex and one of the most common causes of medication resistant epilepsy in pediatric populations, can be studied noninvasively by diffusion tensor imaging (DTI). The present study aimed to quantify changes in the thalamus and thalamocortical pathways with respect to fractional anisotropy (FA), apparent diffusion coefficient (ADC), volume, and other common measures.

Materials and methods: The study quantified data collected from pediatric patients with a prior diagnosis of FCD; 75 patients (35 females, 10.1 ± 6.5 years) for analysis of thalamic volume and 68 patients (32 females, 10.2 ± 6.4 years) for DTI analysis. DTI scans were taken at 3 Tesla MRI scanners (30 diffusion gradient directions; b = 1000 s/mm^2 and 5 non diffusion-weighted measurements). DTI tractography was performed using the FACT algorithm with an angle threshold of 45 degrees. Manually delineated ROIs were used to compare the hemisphere containing the dysplasia to the contralateral hemisphere and controls.

Results: A significant decrease in the volume of the FCD hemisphere thalamus was detected as compared to the contralateral hemisphere. In comparison to controls, there was an observed reduction in tract volume, length, count, FA of thalami, and FA of thalamocortical pathways in FCD patients. FCD patients had higher odds of exhibiting high ADC in both the thalamus and thalamocortical pathways.

Conclusion: The data implied a widespread reduction in structural connectivity of the thalamocortical network. MRI analysis suggests a potential influence of FCD on thalamic volume.

1. Introduction

Focal cortical dysplasia (FCD), a congenital malformation, is thought to be caused by disordered neuronal migration, maturation, and differentiation (Crino and Eberwine, 1997; Eriksson et al., 2001), though the precise etiology remains unclear. Morphologically, the disorder exhibits abnormal neuronal aggregations misplaced in cortical or subcortical regions. FCD is characterized by organizational abnormalities such as neurons misaligned relative to the expected radial orientation, and abnormal structural features of neurons, including a distinct reduction in myelin content (Barkovich et al., 1997; Crino and Eberwine, 1997; Leach et al., 2014; Mellerio et al., 2012; Mühlebner et al., 2012; Taylor et al., 1971). FCD is widely accepted to be the most common cause of pharmacoresistant epilepsy in pediatric populations (Fauser et al., 2014; Harvey et al., 2008; Mellerio et al., 2012; Sisodiya, 2003).

One of the most common and consistent techniques for diagnosing FCD is the use of MRI. Studies have correlated MRI abnormality-driven resection with a reduction in frequency of seizures (Leach et al., 2014; Mühlebner et al., 2012), particularly with complete resection of the epileptogenic region determined by MRI (Chen et al., 2014; Jin et al., 2016; Rowland et al., 2012). MRI findings in FCD include a blurring of the gray and white matter boundary, increased white matter signal, the transmantle sign (an extension of the white matter signal in the direction of the lateral ventricle), and a reduction in focal gray and white matter volume.

Abbreviations: ADC, apparent diffusion coefficient; DTI, diffusion tensor imaging; EMR, electronic medical record; FA, fractional anisotropy; FCD, focal cortical dysplasia; ROI, region of interest.

* Corresponding author at: Division of Newborn Medicine, Department of Medicine, Boston Children's Hospital, Harvard Medical School, 1 Autumn St. #456, Boston, MA 02115, USA.

E-mail address: Emi.Takahashi@childrens.harvard.edu (E. Takahashi).

https://doi.org/10.1016/j.brainres.2018.05.005
0006-8993/

Studies that reported DTI irregularities in FCD have proposed the capability for the technique to detect abnormal connectivity and myelination in the brain (Gross et al., 2005; Lee et al., 2004). DTI relies on the assumption that myelinated axons will prevent isotropic diffusion (the ability for water to move freely in all directions) by restricting water diffusivity perpendicular to the membrane, resulting in a reduction of radial diffusivity compared to longitudinal (axial) diffusivity (anisotropic diffusion). A measure of fractional anisotropy (FA) can therefore suggest if water in a region of the brain diffuses non-uniformly. Myelinated axons and other tissue may also alter the rate of diffusivity of water in a sample, altering their ADC. Thus, measures of water diffusivity by FA and ADC are often used in neuroscientific research and may provide useful information about the location and properties of fiber bundles. DTI tractography, though unable to directly show specific axons and glial fibers, allows us to infer fiber pathways based on water diffusivity.

FCD has been shown to exhibit a decrease in FA in certain white matter tracts (Lee et al., 2004; Wieshmann et al., 1999), likely due to a decrease in myelination in the studied region, which is consistent with histology of FCD brains (Barkovich et al., 1997; Eriksson et al., 2001; Gross et al., 2005; Mühlebner et al., 2012). The present study aims to quantify abnormalities in thalamic volume and thalamocortical pathways in pediatric FCD patients using structural MRI and DTI tractography. Thalamocortical pathways have been found to be well developed and functional in neonatal life (Alcauter et al., 2014; Molnár et al., 2003), and DTI has shown microstructural arrangement of this fiber pathway (Jaermann et al., 2008; Johansen-Berg et al., 2005; Zhang et al., 2010).

2. Results

We confirmed that each DTI measure (thalamocortical tract volume, thalamocortical tract count, thalamocortical tract length, thalamocortical FA, thalamocortical ADC, thalamic FA, thalamic ADC) differed significantly among the three hemisphere classes ($p < 0.05$, 2 degrees of freedom). The principle of closed testing then permitted us to make pairwise comparisons between hemisphere classes without reducing the critical p-value, while preserving the familywise Type I error rate at 0.05 for each measure (Bender and Lange, 2001).

2.1. Hemispheric asymmetry in thalamic volumes

Controls exhibited more symmetric volume measurements, with asymmetry index nearer to zero (median 0, $p = 0.70$ by signed-rank test), than patients, who had a wider distribution and higher values (median 0.011, $p < 0.001$). The difference remained significant after adjustment for sex and age (Fig. 1).

2.2. Volume of the thalamus

Neither the volume of the FCD thalamus nor the contralateral thalamus were significantly different from matched controls ($p = 0.10$ and $p = 0.48$, respectively) (Fig. 2), although both thalami in patients with FCD had a lower average volume than healthy controls (FCD hemisphere < contralateral hemisphere < control) (Fig. 2). Prominent volume reduction was observed in the thalamus of the hemisphere containing the dysplasia when compared to the contralateral thalamus ($p < 0.001$) of patients.

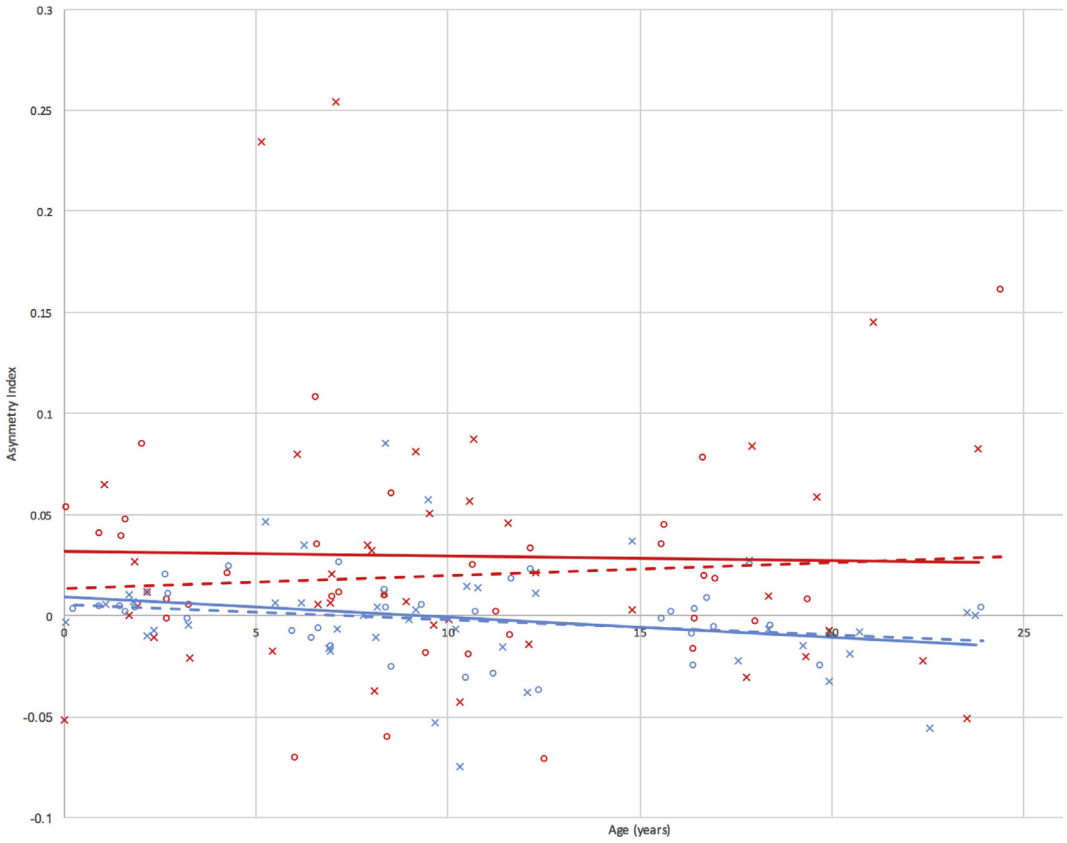

Fig. 1. Scatter Plot of Thalamic Volume Asymmetry Indices in Patients and Controls. Data is displayed according to patients with FCD (red) and controls (blue) as well as males (X) and females (O). FCD is characterized by greater variance in volume between thalami in young ages and overall higher asymmetry indices.

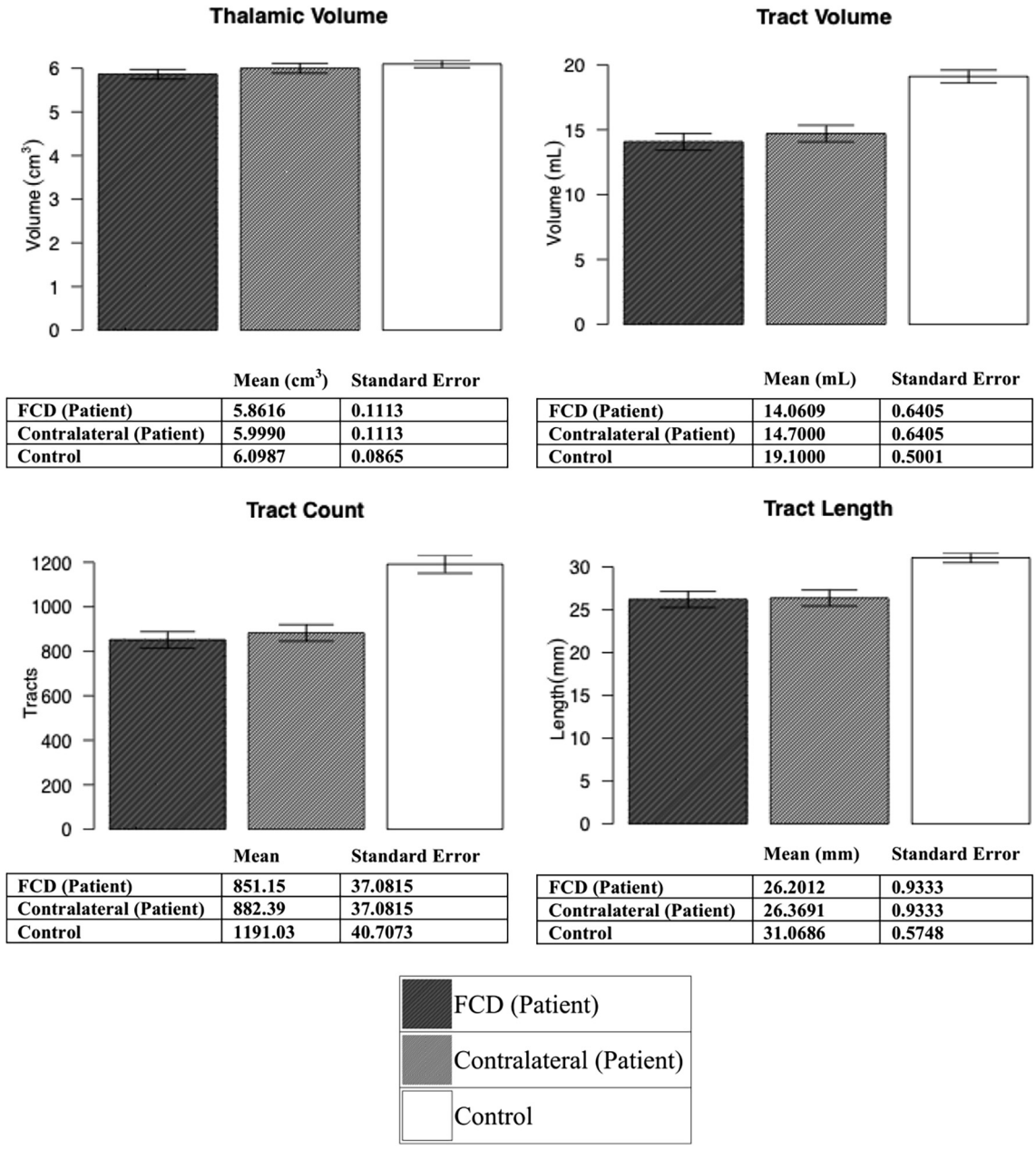

	Mean (cm^3)	Standard Error
FCD (Patient)	5.8616	0.1113
Contralateral (Patient)	5.9990	0.1113
Control	6.0987	0.0865

	Mean (mL)	Standard Error
FCD (Patient)	14.0609	0.6405
Contralateral (Patient)	14.7000	0.6405
Control	19.1000	0.5001

	Mean	Standard Error
FCD (Patient)	851.15	37.0815
Contralateral (Patient)	882.39	37.0815
Control	1191.03	40.7073

	Mean (mm)	Standard Error
FCD (Patient)	26.2012	0.9333
Contralateral (Patient)	26.3691	0.9333
Control	31.0686	0.5748

Fig. 2. Summary of Statistical Analysis for Structural Measures. Bar graphs depict average measures for thalamic volume, tract volume, tract count, and tract length with respect to thalamocortical tracts. Data is displayed according to the hemisphere containing the dysplasia (dark grey), the contralateral hemisphere (light grey), and controls (white). FCD is characterized by a reduction in all measures.

2.3. Thalamocortical tract volume and length

Thalamocortical fibers in the FCD hemisphere, as well as the contralateral hemisphere, displayed a significant reduction in volume ($p < 0.001$ and $p < 0.001$, respectively) when compared to controls (Fig. 3). Tract length of the thalamocortical fibers displayed a similar pattern, with a significant difference between the FCD hemisphere and matched controls ($p < 0.001$ for both tract count and length) and between the contralateral hemisphere and matched controls ($p < 0.001$ for both tract count and length) (Fig. 2).

2.4. FA in the thalamus and thalamocortical tracts

Interpretation of FA data reaffirmed previous findings in cases of FCD (Lee et al., 2004; Wieshmann et al., 1999). FA values of thalamocortical tracts in the hemisphere containing the FCD and the contralateral were reduced as compared to healthy controls ($p = 0.02$ and $p = 0.02$, respectively). FA within the thalami were similarly reduced in the hemisphere containing the dysplastic region ($p < 0.001$), as well as the contralateral ($p < 0.001$). However, FA did not differ between the hemispheres of FCD patients with regard to thalamocortical tracts ($p = 0.72$) nor thalami ($p = 0.22$) (Fig. S1).

2.5. ADC in the thalamus and thalamocortical Tract: Probability-based analysis

Though thalamocortical tract ADC analysis did not show a significant difference between the FCD and contralateral hemispheres in patients ($p = 0.31$, odds ratio of 1.06), the hemisphere with FCD

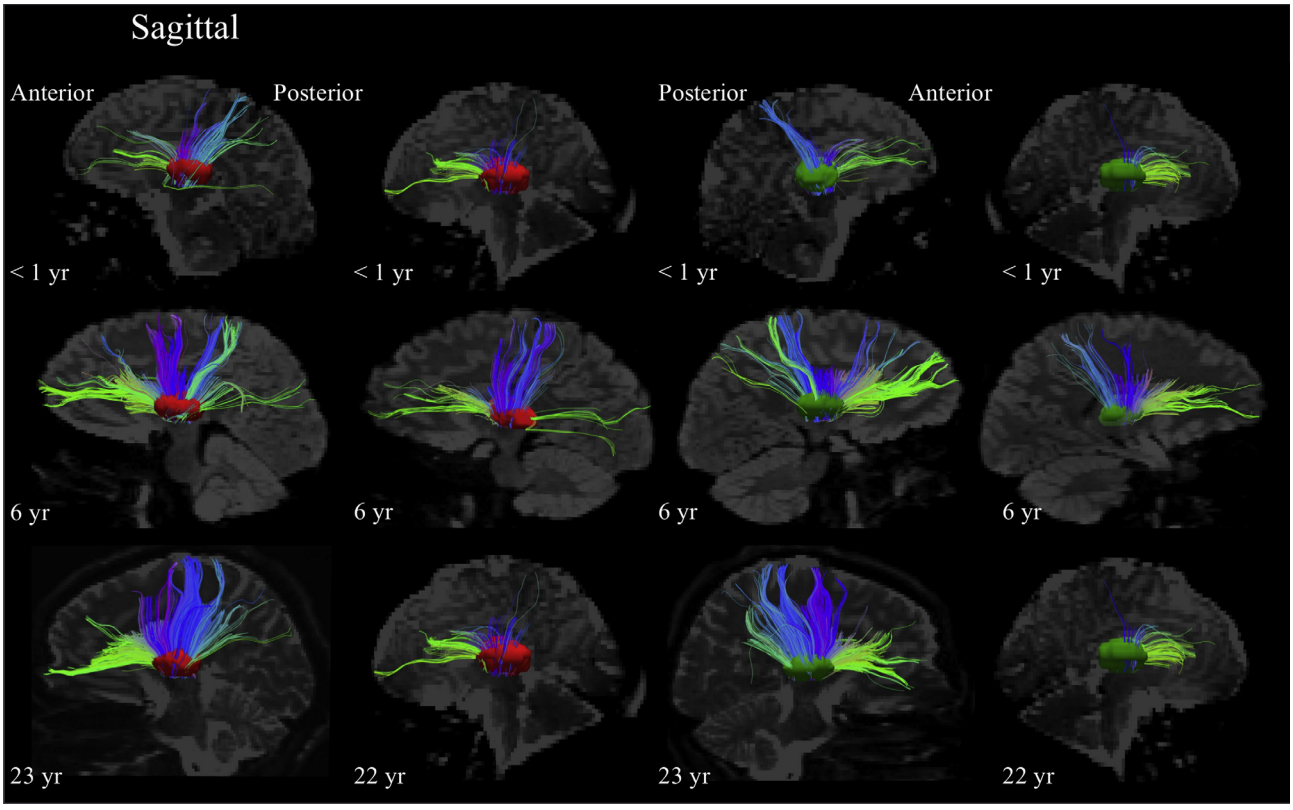

Fig. 3. TrackVis Visualization of Reconstructed Fiber Pathways. Reconstructed fiber pathways are laid over the original DTI for the left thalamus (red) and right thalamus (green) for a healthy control patient (left) and FCD patient (right). Images correspond to different age groups; infants (top, female FCD & control < 1 year), adolescents (middle, male FCD & control 6 years old), and adults (bottom, male FCD 22 years old, control 23 years old). FCD cases are characterized by a visible reduction in reconstructed thalamocortical connectivity.

($p = 0.009$, odds ratio of 2.84) and the contralateral hemisphere ($p = 0.013$, odds ratio of 2.68) both showed a marked increase in the probability of a high ADC value when compared to controls (Fig. S1). Similarly, ADC of the thalamus showed a significant increase in the FCD hemisphere ($p = 0.01$, odds ratio of 2.80) and contralateral hemisphere ($p = 0.01$, odds ratio of 2.68) when compared to controls, but no difference between the FCD hemisphere and contralateral ($p = 0.88$, odds ratio of 1.01). Table 1 shows a numerical summary of statistical analyses.

3. Discussion

This study attempted to quantify DTI measures of the thalamus and thalamocortical pathways in patients with FCD. We compared these quantities between FCD and contralateral hemispheres in patients, as well as between FCD patients and control subjects. The data suggests less structural connectivity between the thalamus and neocortex (thalamocortical pathways) in FCD patients by means of a reduction in tract volume, count, length, FA, and an increase in the probability of high ADC. These results suggest that the measures in the thalamus and thalamocortical pathways can be important biomarkers in patients with FCD.

3.1. Interpretation of findings

The observed reduction in FA may be understood to be a loss of myelin content, as previously observed in FCD through histological study (Barkovich et al., 1997; Mühlebner et al., 2012), however, may also be due to abnormal cellular organization (Crino and Eberwine, 1997), as well as damage to or reduced integrity of white matter microstructures. A reduction in tract volume, count, and length may be due to axonal/fiber damage, lack of axonal/fiber development, or potentially a byproduct of abnormal organization (Sisodiya et al., 1995). Additionally, the increase in probability of high ADC denotes a lack of restriction in water diffusion, which may be due to a loss of myelin content, axonal/fiber damage, lack of axonal/fiber development, or abnormal cellular organization (Gross et al., 2005). Note that though thalamic volume was significantly reduced in the FCD hemisphere as compared to the contralateral hemisphere, there was no significant difference in FA or ADC of the thalamus, nor thalamocortical tracts. This suggests that the observed hemispheric reduction of thalamic volume may not be explained solely by a loss of myelination, as it can be inferred that measures of the properties of water diffusivity (FA and ADC) would be altered. Though studies have quantified FA and ADC in certain brain regions in the past, nearly all literature on DTI imaging in cases of FCD did not use controls in their methodology; rather, statistical measures compared the ipsilateral hemisphere to the contralateral, presupposing that the contralateral is a "healthy" equivalent to control (Diehl et al., 2010; Gross et al., 2005; Lee et al., 2004; Widjaja et al., 2009). As a result, these papers would be unable to detect any potential effects of FCD outside the apparent affected hemisphere; it has been unclear whether inferred neurological detriments exist bilaterally. To the best of our knowledge, there has only been one DTI study on FCD that uses control measures (Fonseca et al., 2012). However, the authors do not provide quantification beyond FA. Prior literature shows many studies are compelled to provide quantification beyond FA to accurately describe abnormal features in the brain by diffusion tensor imaging including ADC (Klimas et al., 2013; Li et al., 2015; Uda et al., 2015), tract count (Catani and Thiebaut de Schotten, 2008; Thiebaut de Schotten et al., 2011), tract volume

Table 1
DTI measures, compared among control subjects and FCD-affected and unaffected hemisphere in patients. Summarizes average values and standard error of measurements regarding thalamic volume, tract volume, tract count, tract length, tract FA, and thalamic FA, as well as probability measures of tract ADC and thalamic ADC. P-values are provided for intra-patient and inter-patient statistical analysis.

Measure	Control	FCD		Contralateral		p†
	Mean ± SE	Mean ± SE	p*	Mean ± SE	p*	
Thalamic volume, cm^3	6.10 ± 0.09	5.86 ± 0.11	0.10	6.00 ± 0.11	0.48	0.0007
Tract volume, mL	19.13 ± 0.50	14.06 ± 0.64	<0.0001	14.70 ± 0.64	<0.0001	0.09
Tract count	1191 ± 41	851 ± 37	<0.0001	882 ± 37	<0.0001	0.25
Tract length, mm	31.1 ± 0.6	26.2 ± 0.9	<0.0001	26.4 ± 0.9	<0.0001	0.77
Tract FA	0.481 ± 0.010	0.450 ± 0.010	0.02	0.448 ± 0.010	0.019	0.72
Thalamic FA	0.363 ± 0.005	0.328 ± 0.007	<0.0001	0.335 ± 0.007	0.0009	0.22
	% High (95% CI)	% High (95% CI)	p*	% High (95% CI)	p*	
Tract ADC, mm^2/s	20 (12–31)	42 (50–34)	0.0088	49 (29–52)	0.0129	0.3068
Thalamic ADC, mm^2/s	18 (11–29)	39 (28–51)	0.0108	38 (27–51)	0.0126	0.8824

* Compared to Control, from factorial ANOVA or logistic regression adjusted for age, sex, and left vs. right hemisphere.
† Comparing FCD to Contralateral.

(Büchel et al., 2004; Eluvathingal et al., 2007; Kulikova et al., 2014; Liu et al., 2010; Takao et al., 2011), and tract length (Baker et al., 2017; Cohen et al., 2016).

3.2. Precision of measure in thalamic volume

Our study found a reduction in thalamic volume in the FCD hemisphere, when compared to the contralateral hemisphere. Although the contralateral hemisphere was not statistically different from the controls, the FCD thalamus did not differ from controls either. This disparity is likely due to the fact that the statistical analysis is dependent on not only the relationships between variables, but the precision with which they are measured; here the contrast between the patients' hemispheres was discernible with high precision due to the intra-patient nature of the comparison. However, the inter-patient contrasts with controls lead to a poor correlation. It becomes clear when analyzing the standard errors for the difference; 0.039 for the FCD to contralateral comparison, and 0.141 for the FCD to control and contralateral to control comparison. Any present signal became more difficult to detect due to noise, however, none of the other measures experienced this issue.

3.3. Thalamic atrophy in demyelinating disorders

Analysis displayed a marked reduction in thalamic volume in FCD. Microstructural thalamic atrophy has previously been observed in another demyelinating disorder, multiple sclerosis (Deppe et al., 2016). Our finding of reduced thalamic volume in FCD suggests that demyelinating disorders may be accompanied by a reduction in thalamic volume, though, our measure of MRI thalamic volume is unable to be directly linked to any DTI findings by this study. However, the basis of correlation between reduction of thalamic volume and demyelinating disorders provides rationale for further study.

3.4. Limitations

Though water diffusivity measures have been analyzed in FCD in the past, we were unable to find prior mention of quantification of a reduction in connectivity between the thalamus and neocortex, as well quantification of a reduction in thalamic volume. The thalamus is important in many pathologies resulting in epilepsy. Though our study lacks pathological confirmation, it is rare to obtain this information in living subjects, of which our sample was based on. We have consulted with a licensed neuroradiologist and have been advised that MRI is largely sufficient for the diagnosis of FCD. Additionally, prior literature has also found MRI signal findings to be sufficient indication of FCD (Barkovich et al., 1997; Gross et al., 2005). It is possible that the findings are representative of epilepsy, rather than the specific pathology under study, though, given the criteria of a FCD diagnosis with no comorbid conditions that affect cerebrum connectivity, we must assume an inability to generalize beyond the pathology being studied. The retrospective nature of the study prevented us from minimizing standard error in inter-subject analyses with regard to thalamic volume. Our study experienced another limitation with respect to the subjective nature of imaging analysis, although this parallels clinical practice. Though DTI imaging of thalamocortical fibers is consistent with microstructural analysis (Jaermann et al., 2008; Johansen-Berg et al., 2005; Zhang et al., 2010), a histological account would strengthen the present findings. While MRI, DTI, and fiber tractography analysis have proven reliable in isolating aspects of FCD, further characteristics of the disorder must be studied in order to develop the practicality of the technique.

4. Conclusion

The present study aimed to quantify changes in the thalamus and thalamocortical pathways with respect to FA, ADC, volume, and other common measures. Our study found a reduction in the volume of the FCD thalamus as compared to the contralateral hemisphere. A reduction in tract volume, count, and length was observed in FCD patients compared to those in control subjects, suggesting less structural connectivity between the thalamus and neocortex in FCD patients. Prior claims of a loss of myelin content in FCD were supported in this study by a significant reduction in FA in the thalamocortical pathways. A reduction in FA in the thalamus may denote a loss of myelin content, though abnormal cellular organization, as well as damage or a reduction of the integrity of white matter microstructures can potentially explain this measure. Additionally, analysis of the high and low ADC dichotomy showed that FCD patients were more likely to exhibit the high ADC values in both the thalamus and thalamocortical tracts, which could support the observed FA reductions in these structures. By quantifying a reduction in cases of FCD, these measures can potentially be used as biomarkers in diagnosis and treatment.

5. Experimental procedure

5.1. Clinical data

Subjects were included based on an indication of FCD in a patient's electronic medical record (EMR) at our hospital, a result

of clinical diagnosis by a neuroradiologist (Fig. S2). Due to the in vivo nature of clinical data, FCD subtypes as determined by histological confirmation could not be provided. Our sample originally began with 97 patients for volumetric analysis and 77 patients for DTI analysis, however, all patients with comorbid conditions indicated in their EMR that were likely to alter structural connectivity (ganglioglioma, benign neoplasms, subcortical nodular heterotopia, subependymal giant cell astrocytoma, tuberous sclerosis, etc.), post-surgical scans, manually determined poor imaging quality (motion artifacts, lack of T1 structural imaging), file corruption, or software error were excluded. The study continued with preoperative radiological diagnosis scans from 75 patients (35 female, 0–24 years, 10.1 ± 6.5, mean ± SD) for volumetric analysis and 68 patients (32 female, 0–24 years, 10.2 ± 6.4, mean ± SD) for DTI analysis, collected between January of 2008 and February of 2016. Control patients were retrospectively matched for age and sex on the basis of an MRI examination devoid of any structural abnormality, as determined by a neuroradiologist, as well as prior medical history that lacks any indication of neurological issues or genetic disorder (Levman et al. 2017). A summary of relevant clinical information for participants is provided (Table 2).

5.2. MRI data acquisition

Patients were scanned for T1 structural images using clinical 3 Tesla MRI scanners (model: Siemens Medical Systems 3.0T Skyra; Erlangen, Germany). Variability in the pulse sequences employed, including several types of MPRAGE acquisitions, as well as variability in spatial resolution between individuals (1.72–2 mm, 1.72–2 mm, 2–2.2 mm), were controlled for to the best of our ability and addressed below (5.4). Despite this variability in MPRAGE acquisition, all diffusion-weighted measurements ($b = 1000\ s/mm^2$) underwent protocol with 30 diffusion gradient directions and 5 b0 measurements.

5.3. Data reconstruction and processing

Volumetric data was segmented (Fig. S3) and quantified automatically with volBrain (Manjón and Coupé, 2016). Results that failed to properly align ROIs to T1 examinations were excluded (i.e. ROIs that extend outside the cerebrum).

DTI tractography was processed using ITK Snap (Yushkevich et al., 2006) for manual delineation of ROIs. With the thalamus as the seed point, we defined thalamocortical tracts to be any tracts with end points in the thalamus that extend radially towards cortex. ROIs were carefully adjusted to avoid inclusion of other white matter pathways. Additional ROIs, such as the mesencephalon, were used to exclude pathways clearly different (such as the cerebrospinal tract) from the pathway of interest.

DiffusionToolkit and TrackVis (Wang et al., 2007) were used for tract reconstruction, visualization, and quantification (Fig. 3). Given the robust nature of the thalamocortical fibers of interest, DTI was deemed a sufficient technique to image these tracts. Pathways were reconstructed for visualization with a streamline/FACT algorithm and a 45° angle threshold. An FA threshold was not set to terminate tractography pathways (e.g. Song et al., 2015; Takahashi et al., 2012; Wedeen et al., 2008); myelination and crossing fibers in post-natal premature brains may result in low FA measures that tend to erroneously terminate tractography pathways. Tractography pathways were reconstructed on a standard red-greenblue (RGB) code which visualizes the spatial orientation of terminal regions for each tract. Red was indicative of left-right, green of anterior-posterior, and blue of dorsal-ventral.

Table 2
Clinical characteristics of FCD patients and controls in analyses. Describes mean age at time of T1 image acquisition (in years), standard deviation, range, gender, and hemisphere containing the region of FCD as determined by MRI.

	FCD Patients	Controls
Volumetric Data		
Average Age, years	10.1	10.1
Standard Deviation	6.5	6.5
Range, years	0–24.4	0–23.9
% Female	46.7	46.7
% Left Hemisphere Dysplasia	48	N/a
	FCD Patients	Controls
DTI Data		
Average Age, years	10.2	10.2
Standard Deviation	6.4	6.4
Range, years	0–24.4	0–23.9
% Female	47.1	47.1
% Left Hemisphere Dysplasia	48.5	N/a

5.4. Quantification

Raw thalamic volume, as provided by volBrain, was transformed into an asymmetry index in order to normalize the effect of spatial resolution. Spatial resolution, though varying between examinations, affects both hemispheres equally within an exam. Thus, between subjects, variability becomes a negligible factor when comparing differences between the thalamus on the hemisphere containing the dysplasia (ipsilateral hemisphere) with the contralateral hemisphere. Additionally, the use of an asymmetry index allows us to control for the wide variability in brain volume in pediatric populations, given that the ratio between thalami should be consistent despite differences in volume. The asymmetry index was calculated as the ratio of the difference between thalami to their mean:

$$Asymmetry\ Index = \frac{2(Thalamus_{contralateral} - Thalamus_{ipsilateral})}{(Thalamus_{contralateral} + Thalamus_{ipsilateral})}$$

Seven program-assessed quantities were recorded; volume, tract count, mean length, FA and ADC of thalamocortical tracts, and FA and ADC of the thalamus.

5.5. Statistical analysis

We compared DTI measures between patients and controls using factorial ANOVA. The unit of analysis was the hemisphere, classified into three groups: FCD-affected in patients; contralateral (unaffected) in patients; and control (two per subject). We accounted for correlation between hemispheres in a given subject by including a random effect in the statistical model, allowing for differing correlation in male and female patients and controls. The ANOVA was also adjusted for sex, age, side (left vs. right hemisphere), and interactions between sex and the other covariates in order to minimize standard error in quantitative analysis. From parameters of the fitted model we constructed covariate-adjusted means for each of the three hemisphere classes, as well as pairwise contrasts between the classes. ADC of both the thalamocortical pathways and the thalamus showed a bimodal distribution and was classified as low (<0.004) or high (≥ 0.004), with 80 measurements scoring high and 192 scoring low across patients and controls. Any relationship between variable ADC measures was therefore evaluated based on an odds ratio. The dichotomous measure was analyzed by logistic regression with a factorial model similar to the ANOVA detailed above. All computations were conducted with SAS software (version 9, Cary, NC). Visual representations of data were reconstructed using the statistical program R (http://www.R-project.org/).

Acknowledgements

This work was supported by the Eunice Shriver Kennedy National Institute of Child Health and Human Development (NICHD) R01HD078561 (ET) and the National Institute of Neurological Disorders and Stroke (NINDS) R03NS091587 (ET). This work was also supported by a Natural Science and Engineering Research Council of Canada's Canada Research Chair grant (231266), a Canada Foundation for Innovation and Nova Scotia Research and Innovation Trust infrastructure grant (R0176004), and a St. Francis Xavier University research startup grant (grant number R0168020) (J.L). The content of the manuscript is the view of the authors and does not necessarily represent the official views of the Eunice Shriver Kennedy NICHD or NINDS. We thank Lana Vasung for valuable technical assistance.

Appendix A. Supplementary data

Supplementary data associated with this article can be found, in the online version, at https://doi.org/10.1016/j.brainres.2018.05.005.

References

Alcauter, S., Lin, W., Smith, J.K., Short, S.J., Goldman, B.D., Reznick, J.S., Gilmore, J.H., Gao, W., 2014. Development of thalamocortical connectivity during infancy and its cognitive correlations. J Neurosci. 34, 9067–9075.

Baker, L.M., Laidlaw, D.H., Cabeen, R., Akbudak, E., Conturo, T.E., Correia, S., Tate, D. F., Heaps-Woodruff, J.M., Brier, M.R., Bolzenius, J., Salminen, L.E., Lane, E.M., McMichael, A.R., Paul, R.H., 2017. Cognitive reserve moderates the relationship between neuropsychological performance and white matter fiber bundle length in healthy older adults. Brain Imaging Behav. 11 (3), 632–639.

Barkovich, A.J., Kuzniecky, R.I., Bollen, A.W., Grant, P.E., 1997. Focal transmantle dysplasia: a specific malformation of cortical development. Neurology 49 (4), 1148–1152.

Bender, R., Lange, S., 2001. Adjusting for multiple testing: when and how? J. Clin. Epidemiol. 45, 343–349.

Büchel, C., Raedler, T., Sommer, M., Sach, M., Weiller, C., Koch, M.A., 2004. White matter asymmetry in the human brain: a diffusion tensor MRI study. Cereb. Cortex 14, 945–951.

Catani, M., Thiebaut de Schotten, M., 2008. A diffusion tensor imaging tractography atlas for virtual in vivo dissections. Cortex 44, 1105–1132.

Chen, H.H., Chen, C., Hung, S.C., Liang, S.Y., Lin, S.C., Hsu, T.R., Yeh, T.C., Yu, H.Y., Lin, C.F., Hsu, S.P.C., Liang, M.L., Yang, T.F., Chu, L.S., Lin, Y.Y., Chang, K.P., Kwan, S.Y., Ho, D.M., Wong, T.T., Shih, Y.H., 2014. Cognitive and epilepsy outcomes after epilepsy surgery caused by focal cortical dysplasia in children: early intervention maybe better. Childs Nerv. Syst. 30 (11), 1885–1895.

Cohen, A.H., Wang, R., Wilkinson, M., MacDonald, P., Lim, A.R., Takahashi, E., 2016. Development of human white matter fiber pathways: from newborn to adult ages. Int. J. Dev. Neurosci. 50, 26–38.

Crino, P.B., Eberwine, J., 1997. Cellular and molecular basis of cerebral dysgenesis. J. Neurosci. Res. 50 (6), 907–916.

Deppe, M., Krämer, J., Tenberge, J.G., Marinell, J., Schwindt, W., Deppe, K., Groppa, S., Wiendl, H., Meuth, S.G., 2016. Early silent microstructural degeneration and atrophy of the thalamocortical network in multiple sclerosis. Hum. Brain Mapp. 37 (5), 1866–1879.

Diehl, B., Tkach, J., Piao, Z., Ruggieri, P., Lapresto, E., Liu, P., Fisher, E., Bingaman, W., Naim, I., 2010. Diffusion tensor imaging in patients with focal epilepsy due to cortical dysplasia in the temporo-occipital region: electro-clinico-pathological correlations. Epilepsy Res. 90 (3), 178–187.

Eluvathingal, T.J., Hasan, K.M., Kramer, L., Fletcher, J.M., Ewing-Cobbs, L., 2007. Quantitative diffusion tensor tractography of association and projection fibers in normally developing children and adolescents. Cereb. Cortex 17, 2760–2768.

Eriksson, S.H., Rugg-Gunn, F.J., Symms, M.R., Barker, G.J., Duncan, J.S., 2001. Diffusion tensor imaging in patients with epilepsy and malformations of cortical development. Brain 124 (3), 617–626.

Fauser, S., Essang, C., Altenmuller, D.M., Staack, A.M., Steinhoff, B.J., Strobl, K., Bast, T., Schubert-Bast, S., Stephani, U., Wiegand, G., Prinz, M., Brandt, A., Zentner, J., Schulze-Bonhage, A., 2014. Long-term seizure outcome in 211 patients with focal cortical dysplasia. Epilepsia 56 (1), 66–76.

Fonseca, V.D.C., Yasuda, C.L., Tedeschi, G.G., Betting, L.E., Cendes, F., 2012. White matter abnormalities in patients with focal cortical dysplasia revealed by diffusion tensor imaging analysis in a voxelwise approach. Front. Neurol. 3, 121.

Gross, D.W., Bastos, A., Beaulieu, C., 2005. Diffusion tensor imaging abnormalities in focal cortical dysplasia. Can. J. Neurol. Sci. 32 (4), 477–482.

Harvey, A.S., Cross, J.H., Shinnar, S., Mathern, G.W., 2008. Defining the spectrum of international practice in pediatric epilepsy surgery patients. Epilepsia 49 (1), 146–155.

Jaermann, T., De Zanche, N., Staempfli, P., Pruessmann, K.P., Valavanis, A., Boesiger, P., Kollias, S.S., 2008. Preliminary experience with visualization of intracortical fibers by focused high-resolution diffusion tensor imaging. Am. J. Neuroradiol. 29 (1), 146–150.

Jin, B., Wang, J., Zhou, J., Wang, S., Guan, Y., Chen, S., 2016. A longitudinal study of surgical outcome of pharmacoresistant epilepsy caused by focal cortical dysplasia. J. Neurol. 263 (12), 2403–2410.

Johansen-Berg, H., Behrens, T.E.J., Sillery, E., Ciccarelli, O., Thompson, A.J., Smith, S. M., Matthews, P.M., 2005. Functional-anatomical validation and individual variation of diffusion tractography-based segmentation of the human thalamus. Cereb. Cortex 15, 31–39.

Klimas, A., Drzazga, Z., Kluczewska, E., Hartel, M., 2013. Regional ADC measurements during normal brain aging in the clinical range of b values: a DWI study. Clin. Imaging 37, 637–644.

Kulikova, S., Hertz-Pannier, L., Dehaene-Lambertz, G., Buzmakov, A., Poupon, C., Dubois, J., 2014. Multi-parametric evaluation of the white matter maturation. Brain Struct. Funct. 220 (6), 3657–3672.

Leach, J.L., Greiner, H.M., Miles, L., Mangano, F.T., 2014. Imaging spectrum of cortical dysplasia in children. Semin. Roentgenol. 49 (1), 99–111.

Lee, S.K., Kim, D.I., Mori, S., Kim, J., Kim, H.D., Heo, K., Lee, B., 2004. Diffusion tensor MRI visualizes decreased subcortical fiber connectivity in focal cortical dysplasia. Neuroimage 22 (4), 1826–1829.

Levman, J., MacDonald, P., Lim, A.R., Forgeron, C., Takahashi, E., 2017. A pediatric structural MRI analysis of healthy brain development from newborns to young adults. Hum. Brain Mapp. 38 (12), 5931–5942.

Li, H., Jiang, X., Wang, F., Xu, J., Gore, J.C., 2015. Structural information revealed by the dispersion of ADC with frequency. Magn. Reson Imaging 33, 1083–1090.

Liu, Y., Balerjaux, D., Kavec, M., Metens, T., Absil, J., Denolin, V., Pardou, A., Avni, F., Van Bogaert, P., Aeby, A., 2010. Structural asymmetries in motor and language networks in a population of healthy preterm neonates at term equivalent age: a diffusion tensor imaging and probabilistic tractography study. Neuroimage 51, 783–788.

Manjón, J.V., Coupé, P., 2016. volBrain: an online brain volumetric system. Front. Neuroinf. 10, 30.

Mellerio, C., Labeyrie, M.A., Chassoux, F., Daumas-Duport, C., Landre, E., Turak, B., Roux, F.X., Meder, J.F., Devaux, B., Oppenheim, C., 2012. Optimizing MR imaging detection of type 2 focal cortical dysplasia: best criteria for clinical practice. Am. J. Neuroradiol. 33 (10), 1932–1938.

Molnár, Z., Higashi, S., López-Bendito, G., 2003. Choreography of early thalamocortical development. Cereb. Cortex 13, 661–669.

Mühlebner, A., Coras, R., Kobow, K., Feucht, M., Czech, T., Stefan, H., Weigel, D., Buchfelder, M., Holthausen, H., Pieper, T., Kudernatsch, M., Blümcke, I., 2012. Neuropathologic measurements in focal cortical dysplasias: validation of the ILAE 2011 classification system and diagnostic implications for MRI. Acta Neuropathol. 123 (2), 259–272.

Rowland, N.C., Englot, D.J., Cage, T.A., Sughrue, M.E., Barbaro, N.M., Chang, E.F., 2012. A meta-analysis of predictors of seizure freedom in the surgical management of focal cortical dysplasia. J. Neurosurg. 116 (5), 1035–1041.

Sisodiya, S.M., 2003. Malformations of cortical development: burdens and insights from important causes of human epilepsy. Lancet Neurol. 3 (1), 29–38.

Sisodiya, S.M., Free, S.L., Stevens, J.M., Fish, D.R., Shorvon, S.D., 1995. Widespread cerebral structural changes in patients with cortical dysgenesis and epilepsy. Brain 118, 1039–1050.

Song, J.W., Mitchell, P.D., Kolasinski, J., Ellen-Grant, P., Galaburda, A.M., Takahashi, E., 2015. Asymmetry of white matter pathways in developing human brains. Cereb. Cortex 25, 2883–2893.

Takahashi, E., Folkerth, R.D., Galaburda, A.M., Grant, P.E., 2012. Emerging cerebral connectivity in the human fetal brain: an MR tractography study. Cereb. Cortex 22, 455–464.

Takao, H., Abe, O., Yamasue, H., Aoki, S., Sasaki, H., Kasai, K., Yoshioka, N., Ohtomo, K., 2011. Gray and white matter asymmetries in healthy individuals aged 21–29 years: a voxel-based morphometry and diffusion tensor imaging study. Hum. Brain Mapp. 32, 1762–1773.

Taylor, D.C., Falconer, M.A., Bruton, C.J., Corsellis, J.A., 1971. Focal dysplasia of the cerebral cortex in epilepsy. J. Neurol. Neurosurg. Psychiatry 34 (4), 369–387.

Thiebaut de Schotten, M., Ffytche, D.H., Bizzi, A., Dell'Acqua, F., Allin, M., Walshe, M., Murray, R., Williams, S.C., Murphy, D.G., Catani, M., 2011. Atlasing location, asymmetry and inter-subject variability of white matter tracts in the human brain with MR diffusion tractography. Neuroimage 54, 49–59.

Uda, S., Matsui, M., Tanaka, C., Uematsu, A., Miura, K., Kawana, I., Noguchi, K., 2015. Normal development of human brain white matter from infancy to early adulthood: a diffusion tensor imaging study. Dev. Neurosci. 37 (2), 182–194.

Wang, R., Benner, T., Sorensen, A.G., Wedeen, V.J., 2007. Diffusion Toolkit: a software package for diffusion imaging data processing and tractography. Proc. Intl. Soc. Mag. Reson. Med. 15, 3720.

Wedeen, V.J., Wang, R.P., Schmahmann, J.D., Benner, T., Tseng, W.Y.I., Dai, G., Pandya, D.N., Hagmann, P., D'Arceuil, H., de Crespigny, A.J., 2008. Diffusion spectrum magnetic resonance imaging (DSI) tractography of crossing fibers. Neuroimage 41, 1267–1277.

Widjaja, E., Zarei Mahmoodabadi, S., Otsubo, H., Snead, O.C., Holowka, S., Bells, S., Raybaud, C., 2009. Subcortical alterations in tissue microstructure adjacent to focal cortical dysplasia: detection at diffusion-tensor MR imaging by using magnetoencephalographic dipole cluster localization. Radiology 251 (1), 206–215.

Wieshmann, U.C., Clark, C.A., Symms, M.R., Franconi, F., Barker, G.J., Shorvon, S.D., 1999. Reduced anisotropy of water diffusion in structural cerebral abnormalities demonstrated with diffusion tensor imaging. Magn. Reson. Imaging 17 (9), 1269–1274.

Yushkevich, P.A., Piven, J., Hazlett, H.C., Smith, R.G., Ho, S., Gee, J.C., Gerig, G., 2006. User-guided 3D active contour segmentation of anatomical structures: significantly improved efficiency and reliability. Neuroimage 31 (3), 1116–1128.

Zhang, D., Snyder, A.Z., Shimony, J.S., Fox, M.D., Raichle, M.E., 2010. Noninvasive functional and structural connectivity mapping of the human thalamocortical system. Cereb. Cortex 20, 1187–1194.